ELSEVIER

Journal of Nuclear Materials 241–243 (1997) 993–997

journal of nuclear materials

Wall conditioning and particle control in Extrap T2

H. Bergsåker [b,*], D. Larsson [b], P. Brunsell [a], A. Möller [a], L. Tramontin [c]

[a] *Department of Fusion Plasma Physics, Alfvén Laboratory, Royal Institute of Technology, EURATOM / NFR Fusion Association, 100 44 Stockholm, Sweden*

[b] *Department of Physics Frescati, Royal Institute of Technology, EURATOM / NFR Fusion Association, 104 05 Stockholm, Sweden*

[c] *Dipartimento di Ingegneria Elettrica, Università di Padova, Padua, Italy*

Abstract

The Extrap T2 reversed field pinch experiment is operated with the former OHTE vacuum vessel, of dimensions $R = 1.24$ m and $a = 0.18$ m and with a complete graphite liner. It is shown that a rudimentary density control can be achieved by means of frequent helium glow discharge conditioning of the wall. The standard He-GDC is well characterized and reproducible. The trapping and release of hydrogen and impurities at the wall surfaces have been studied by mass spectrometry and surface analysis. The shot to shot particle exchange between wall and plasma can be approximately accounted for.

Keywords: EXTRAP-T2; Boundary plasma; Reversed field pinch; Wall pumping; Wall conditioning

1. Introduction

The Extrap T2 experiment aims at improvements of the reversed field pinch concept with resistive shell operation [1]. In its first stage, the experiment is operated with the former OHTE vacuum vessel with a complete graphite liner [2,3]. One target has been to reproduce the OHTE results, though with improved diagnostic facilities. Another major objective has been to study plasma surface interactions and methods of density control and impurity control with a graphite wall [4,5].

The dimensions of T2 are major radius $R = 1.24$ m and minor radius $a = 0.183$ m. The global plasma parameters so far have been in the ranges of 100–260 kA plasma current, $1\text{–}7 \cdot 10^{19}$ m^{-3} line averaged density and 100–200 eV electron temperature. The loop voltage has been 70–130 V, the pulse length 4–14 ms and the energy confinement time 50–80 μs. These data are comparable to the OHTE performance [2,3].

The main tools for wall conditioning have been glow discharges in helium, baking and conditioning by repeated RFP discharges. To study the effects of these procedures on the wall surfaces, quantitative mass spectrometry and surface analysis of passive probes have been used.

2. Experimental

The T2 device has normally been operated at room temperature. It is routinely baked up to ~ 130°C, each time for about eight hours. The base pressure is around 10^{-5} Pa. The effective pumping speed on the vessel is limited by the size of the pump ports to roughly $S \approx 0.25$ m^3/s at base pressure, $S = 0.175$ m^3/s at 0.5 Pa. At an earlier stage the discharge gas was supplied in continuous flow, to a vessel pressure of 0.1–0.7 Pa. Later, gas puffs of ~ 20 s duration were introduced. For hydrogen removal and cleaning an rf assisted dc glow discharge in helium at room temperature with a single recessed anode has been used [4]. A glow which is toroidally uniform within a factor two can be obtained at a pressure of ~ 0.7 Pa, with ~ 650 V anode potential and an average current density of 80 mA/m^2 wall area [4]. These parameters will be referred to below as the standard He-GDC. Occasionally a glow discharge in hydrogen with similar parameters, followed by a He-GDC has been made in order to remove oxygen more efficiently.

* Corresponding author.

PII S0022-3115(96)00646-0

The edge plasma density and temperature were measured with a Langmuir triple probe of similar geometry as in [6]. A quadrupole mass spectrometer mounted directly on the vessel could be operated up to a total pressure of $\sim 10^{-2}$ Pa. Another, differentially pumped mass spectrometer was calibrated for N_2, H_2 and He in the range of vessel pressure from 0.1–10 Pa. A probe manipulator system allows passive probes to be exposed to complete RFP discharges or to wall conditioning. Following exposure the probes are transferred via a portable UHV cassette to either of two surface analysis stations, for ion beam analysis or for X-ray photoelectron spectroscopy and scanning Auger electron spectrometry. In particular, graphite and silicon probes have been exposed at the wall position and in slightly retracted positions. The samples have been transported at 10^{-4} Pa or better, and surface analysis could be performed typically within a few hours after exposure.

3. Results

Fig. 1 shows the plasma current and density evolution in three representative examples of RFP discharges. Characteristic is the wide range of different densities that can occur, depending on the status of the graphite wall. Shot number 2531 was preceded by a 60 min glow discharge in helium. The density increase which is observed from around $t = 3$ ms in these three discharges is representative and is often accompanied by an increase in radiation from carbon and oxygen and an increase in plasma resistance. Fig. 2 shows the edge temperature and edge density at the time of maximum current as a function of line averaged

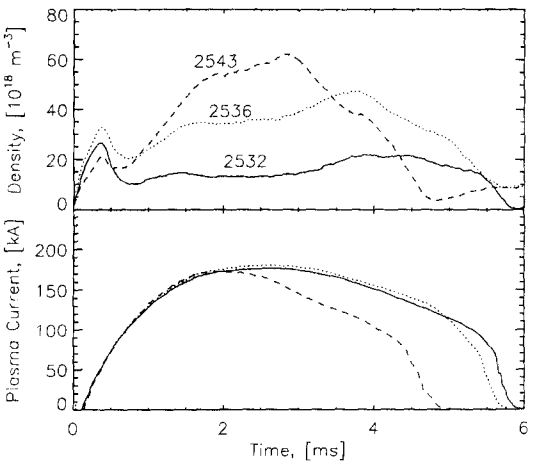

Fig. 1. Examples of current wave form and density evolution in RFP discharges. Shot number 2531 was preceded by a glow discharge in He. The density rise at around $t = 3$ ms is interpreted as being due to an increased impurity influx, probably as a result of local heating.

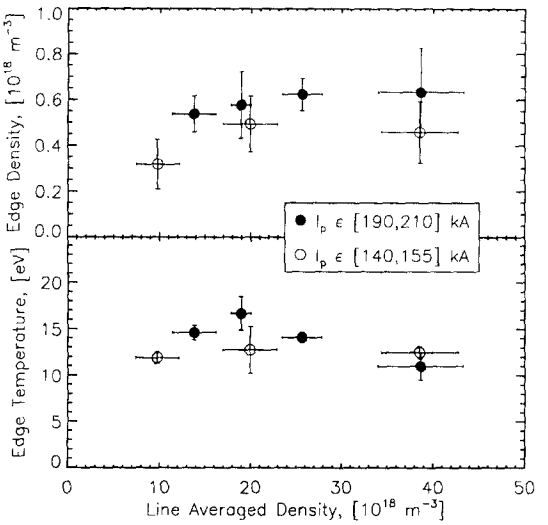

Fig. 2. The edge density and edge temperature from Langmuir triple probe measurements. The data for the lower currents are taken at $r = 0.181$ m, while the high current measurements were made at $r = 0.179$ m. At these positions the density and temperature drop radially on the scale length of $\lambda \approx 8$ mm. The edge parameters depend only weakly on the line averaged density and plasma current.

density in high and low current discharges respectively. The edge parameters depended only weakly on the central density, and there was no significant dependence on the plasma current either. The edge temperature was 10–18 eV.

That the graphite wall pumps hydrogen during the discharge is evident from Fig. 3, where a typical pressure decrement in connection to an RFP discharge is shown. In this case the gas supply is set to constant gas flow. During the plasma discharge the pressure drops by $\Delta p \approx 0.12$ Pa, corresponding to $N = 2\Delta pV/kT \approx N \sim 5 \cdot 10^{19}$ hydrogen

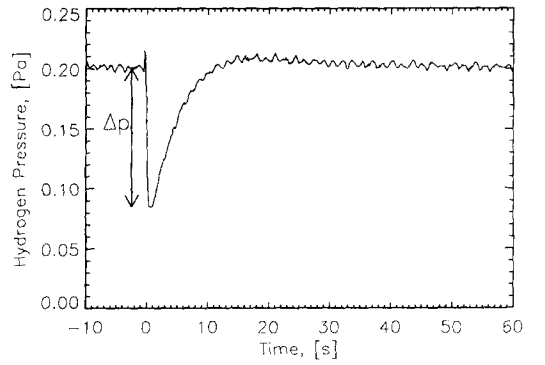

Fig. 3. The partial pressure transient in connection with an RFP discharge, the gas supply is set to constant flow control. A trapping rate of $5 \cdot 10^{18}$ H/m^2 per discharge at the wall can be inferred.

atoms being trapped by the wall, then reverts to its equilibrium value on the time scale of the characteristic pump down time $\tau_S = V/S \approx 3$ s. Typically $5 \cdot 10^{18}$ H/m^2 are trapped by the wall in an RFP discharge. Note that some of this hydrogen is released within 10–20 s after the discharge, as evidenced by the slight pressure increase after the discharge, though it is difficult to estimate this fraction accurately.

The amount of hydrogen that is removed in the helium glow discharges has been measured as shown in Fig. 4, where mass spectrometer data are presented for a set of standard helium glow discharges, following similar series of RFP discharges. There is an increment $\Delta p_g(t)$ in the hydrogen partial pressure while the glow discharge is on, corresponding to a flux of hydrogen being released from the wall. The time dependence of the release can be fitted quite well to be proportional to $t^{-0.9}$. Integrated over the glow discharge the number of hydrogens which have been released from the wall and pumped out was calculated as

$$\Delta N_w = 2 \cdot \int \frac{\Delta p_g S}{kT} dt \quad (1)$$

and for the standard situation shown in the figure $\Delta N_w/A \approx 1.5 \cdot 10^{20}$ H/m^2 wall area were removed.

Usually sequences of 10–30 RFP discharges have been run, each sequence terminated with a standard He-GDC. In operating this way the standard He-GDC was capable of restoring the wall surface to the original state as far as plasma density is concerned. This is shown in Fig. 5, which presents the shot to shot density evolution averaged between glow discharges. The discharge duration was 6 ms. Each point in the figure represents an average over 5–15 discharge sequences. The bars indicate the statistical standard deviation and are drawn only for the medium current discharges, while the scatter among the high and low current discharges is similar. The densities at the point of maximum current are plotted, which is prior to the final density increase (cf. Fig. 1). There is no significant difference between the 150–170 kA sequences and the 170–200 kA case, but in the 100–140 kA sequences the density

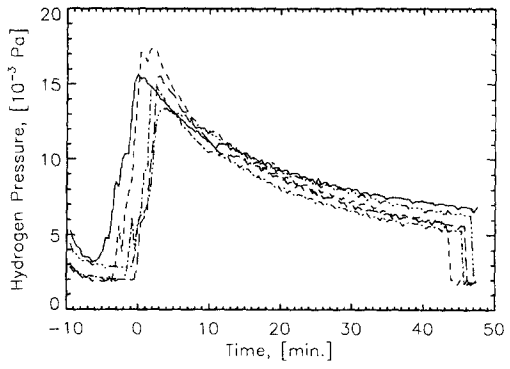

Fig. 4. The partial pressure evolution of hydrogen during the standard glow discharges in helium. In the 45 min standard helium glow $1.5 \cdot 10^{20}$ H/m^2 are removed.

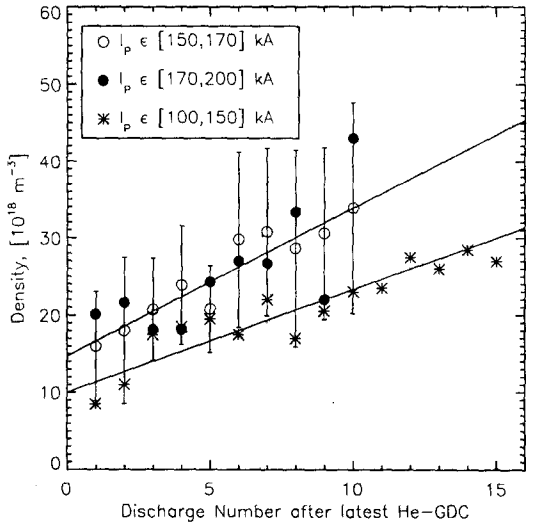

Fig. 5. The evolution from shot to shot of the line averaged density at maximum current in a number of discharge sequences following helium glow discharges. The bars which are drawn for the medium current data indicate the statistical standard deviation. The scatter is similar for the high and low current discharges.

increase is slower. The low current sequences correspond largely to the glow discharges which are plotted in Fig. 4.

Fig. 6 shows examples of impurity accumulation on

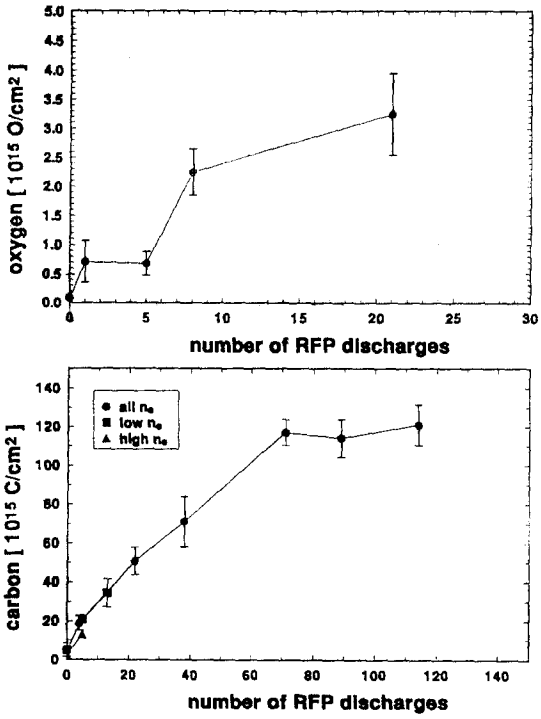

Fig. 6. The trapping of oxygen in a 30 nm thick surface layer of a graphite surface and the collection of carbon at a silicon surface, both at wall radius.

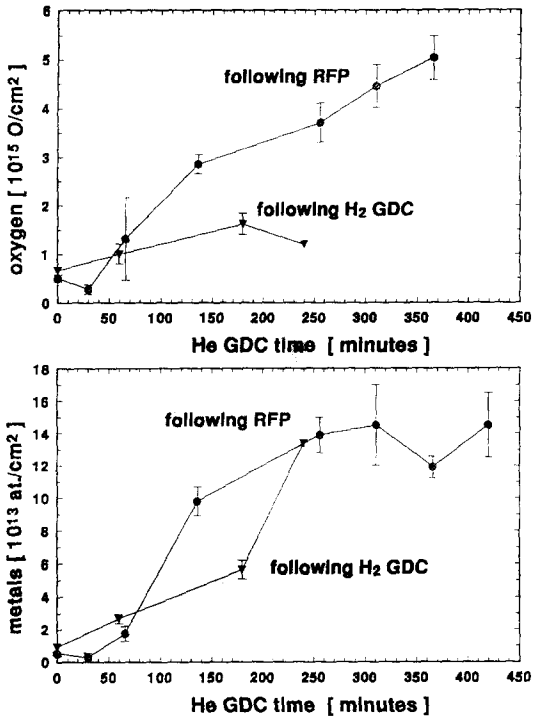

Fig. 7. The trapping of oxygen and stainless steel components on graphite at wall radius.

initially clean surfaces which have been exposed at the wall position to long sequences of RFP discharges, but without exposure to the intervening He-GDC. The upper part shows the areal density of oxygen trapped within a 30 nm thick layer on graphite surface, whereas the lower part shows carbon accumulation on a silicon surface. Similarly Fig. 7 shows the accumulation of oxygen and stainless steel components in helium glow discharges which follow RFP operation and glow discharges in hydrogen, respectively. In all cases the trapping rate is initially linear with exposure time, and may or may not tend towards a stationary equilibrium areal density. In RFP discharges representative initial trapping rates at the wall position have been $2.5 \cdot 10^{19}$ C/m^2, $2.5 \cdot 10^{18}$ O/m^2, and $3 \cdot 10^{16}$ metal-atoms/m^2 per discharge. Other accumulating impurities have been nitrogen, chlorine and silicon. The small amounts of stainless steel which are present on the wall have been built up mostly during a long period of OHTE operation and the primary source can not be identified. For comparison, the initial trapping rate of hydrogen (or deuterium in discharges in deuterium) was typically $5 \cdot 10^{19}$ atoms/m^2 per discharge on carbon or silicon surfaces.

4. Discussion and conclusions

As is well known from ion beam experiments as well as from other large fusion experiments, the graphite wall acts in the first approximation as a saturable reservoir of hydrogen. In the absence of sufficiently large external particle sources, the pumping and release by the wall determines the plasma density. The mass spectrometry and surface probe data can be used for a more quantitative account of the particle exchange between wall and plasma. The initial trapping rate of deuterium in pure graphite, $5 \cdot 10^{19}$ D/m^2 per discharge, can be taken to represent roughly the incident flux density of hydrogen to the wall [7] and corresponds to a particle confinement time of roughly 150 μs. From Fig. 3 it was seen that the partially saturated wall traps $5 \cdot 10^{18}$ H/m^2 per discharge.

The effectiveness of He glow discharge in removing hydrogen from carbon surfaces has been qualitatively demonstrated before, in several large fusion experiments, such as OHTE [3], TEXTOR [8], DIII-D [9] and JT-60U [10]. As shown in Fig. 4, the standard He-GDC in T2 removed $1.5 \cdot 10^{20}$ H/m^2 following 10–30 low current discharges, which corresponds reasonably well to the 0.5–$1.5 \cdot 10^{20}$ H/m^2 that the wall has trapped. The release mechanism of hydrogen during helium ion bombardment, in particular in a glow discharge, has not been as extensively discussed in the literature as the trapping, release and isotopic exchange during hydrogen implantation. The time dependence of $\Delta p_g(t)$ as shown in Fig. 4 can be compared to a numerical model which was developed for Tore Supra [11] and which included ion induced detrapping with a fixed cross section, thermal detrapping, diffusion and surface as well as bulk recombination. The present time dependence of $\sim t^{-0.9}$ may be indicative of a intermediate condition between diffusion limited and recombination limited release. In the present case however, thermally activated release is clearly negligible compared to the ion induced release.

That the standard He-GDC removes a substantial fraction of the total wall reservoir of hydrogen which is interacting with the plasma could be seen from an isotopic exchange from ^{1}H to D, when mass spectrometry following the discharges showed a change of the isotopic ratio at a rate of $\sim 5\%$ per shot [5]. Thus a number $N_D = 2p_{fill}V/kT \approx 2 \cdot 10^{20}$ deuterium atoms were admitted as filling gas in every discharge, representing a fraction $F_{fill} = N_D/(N_D + N_w)$ of the total hydrogen content in the system, if $N_w = N_{WD} + N_{WH}$ is the wall reservoir. The deuterium fraction $r_D = N_{WD}/N_w$ in the wall following the first pulse with deuterium would be $r_{D1} = F_{fill}$ and after the ith pulse $r_{Di} = (1 - F_{fill})r_{D(i-1)} + F_{fill}$. This should correspond to the isotope ratio observed in the mass spectrometry, such that $N_W = 20N_D \approx 4 \cdot 10^{21}$ H, or $4 \cdot 10^{20}$ H/m^2. This areal density corresponds to the saturation level of 100 eV deuterium ions implanted into graphite [12].

Carbon and oxygen are the spectroscopically dominating impurities in T2 RFP operation. The collection rates of C and O on initially clean surfaces provide an estimate of their absolute concentrations and Fig. 6 may give an idea

of the rate at which an equilibrium condition is approached at the wall surfaces. Fig. 7 shows that the He-GDC is able to redistribute oxygen. The metals on the wall clearly reach a stationary level after 250 min or so, presumably when sputtering and redeposition balance, but this behavior is not observed for oxygen.

In conclusion, it has been shown that a rudimentary density control could be achieved by means of frequent helium glow discharge conditioning of the wall. The standard He-GDC is well characterized and reproducible. The hydrogen and impurity trapping at the wall has been measured in RFP discharges and in glow discharges so as to provide a basis for plasma performance to wall conditions. The shot to shot particle exchange between wall and plasma can be approximately accounted for. Fluxes of major impurities are given in terms of initial trapping rates on clean surfaces at the wall position.

References

[1] P. Brunsell, H. Bergsåker, J. Brzozowski et al., Proc. 22nd Eur. Conf. Controlled Fusion Plasma Phys., Bournemouth, UK, July (1995) Part III, p. 157.
[2] R.R. Goforth et al., Nucl. Fusion 26 (1986) 515.
[3] G.L. Jackson, T.S. Taylor, T.N. Carlstrom et al., J. Nucl. Mater. 145–147 (1987) 470.
[4] D. Larsson, H. Bergsåker, B. Emmoth et al., Proc. 18th Symp. Fusion Technol. Karlsruhe, August 22–26 (1994) Vol. 1, p. 207.
[5] H. Bergsåker, P. Brunsell, D. Larsson and L. Tramontin, Proc. 22nd Eur. Conf. Contr. Fusion Plasma Phys. Bournemouth, UK, July (1995) Part IV, p. 277.
[6] H. Bergsåker, A. Möller, G.X. Li et al., J. Nucl. Mater. 220–222 (1995) 712.
[7] W.R. Wampler, D.K. Brice and C.W. Magee, J. Nucl. Mater. 102 (1981) 304.
[8] F. Waelbroeck, T. Banno, H.G. Esser et al., J. Nucl. Mater. 162–164 (1989) 496.
[9] G.L. Jackson, T.S. Taylor, S.L. Allen et al., J. Nucl. Mater. 162–164 (1989) 489.
[10] M. Shimada, A. Sakasai, R. Yoshino et al., J. Nucl. Mater. 196–198 (1992) 164.
[11] C. Grisoglia, L.D. Horton and J. Ehrenberg, J. Nucl. Mater. 220–222 (1995) 516.
[12] G. Staudenmaier, J. Roth, R. Behrisch et al., J. Nucl. Mater. 84 (1979) 149.